The lacquer crafting of Ba state: Insights from a Warring States lacquer scabbard excavated from Lijiaba site (Chongqing, southwest China)

Bin Han, Xiaopan Fan, Yun Chen, Jie Gao, Michel Sablier

The lacquer crafting of *Ba* state: insights from a Warring States lacquer scabbard excavated from Lijiaba site (Chongqing, southwest China)

Bin Han[a] , Xiaopan Fan[b*], Yun Chen[c], Jie Gao[d], Michel Sablier[e*],

[a] Department of Archaeology and Anthropology, School of Humanities, University of Chinese Academy of Sciences, 100049 Beijing, China
[b] History and Social Work College, Chongqing Normal University, 401331 Chongqing, China
[c] Yunyang Museum, 404500 Chongqing, China
[d] Shimadzu (China) Co. LTD, 100020 Beijing, China
[e] Centre de Recherche sur la Conservation (CRC, USR 3224), Muséum national d'Histoire naturelle, Ministère de la Culture, CNRS, 75005 Paris, France

[*]corresponding authors：fxiaopan@163.com (X. Fan); michel.sablier@mnhn.fr (M. Sablier)

Abstract: The lacquer scabbard of a bronze sword dating from the Warring States (476-221 BC) and excavated from a *Ba* tomb of the Lijiaba site (Chongqing, southwest China) was characterized by a multidisciplinary approach including microscopy, scanning electron microscopy-energy dispersive X-ray spectrometry (SEM-EDS), Raman spectroscopy and pyrolysis-gas chromatography/mass spectrometry (Py-GC/MS). Pyrolysis-comprehensive two-dimensional gas chromatography/mass spectrometry (Py-GCxGC/MS) has been applied for the first time for the characterization of a valuable archaeological lacquer sample confirming the benefits of this technique for the description of the ingredients used in the formulation of the lacquer coating. Besides, the analytical results also showed that, in accordance with what is suspected from the lacquer technique employed at this period, two lacquer film layers and a bone-derived ground layer were present as confirmed by the characterization of hydroxyapatite particles ($Ca_5(PO_4)_3OH$) of different sizes. Py-GC/MS analysis allowed identification of the origin of the scabbard lacquer as a *Toxicodendron vernicifluum* lacquer and detection of potential drying oil markers, while Py-GCxGC/MS analysis revealed the presence of a series of polyaromatic hydrocarbons (PAHs) compounds non-characterizable by 1D GC/MS analysis. This latter observation highlights the use of soot attributed to a plant origin in conjunction with bone for the manufacture and coloring of the lacquers.

Key words: *Ba* ethnic group, Lijiaba site, lacquer scabbard, Asian lacquer, *Toxicodendron vernicifluum*, Py-GCxGC/MS, PAHs characterization

1. Introduction

Lacquer is a natural product which is polymerized by laccase enzyme and has been used as coating materials for wooden crafts, ceramics, leather and metal artifacts since the Neolithic period (Zhai et al., 2021). Lacquer sap usually contains urushiol, plant gum, laccase, nitrogen substance, and water. Different lacquer trees, depending on their locations of growth, have been traditionally used for lacquer making in the countries where lacquer artworks have been developed (Lu et al., 2012). Globally, the Asian lacquer reported as *shengqi* (in China) and *urushi* (in Japan) is a sap collected from lacquer trees of the *Toxicodendron vernicifluum (Stokes) F. A. Barkley* species, for which the principal component is urushiol (C15 unsaturated hydrocarbon chains at the 3-position of the catechol ring). Vietnam's and Taiwan region's lacquer consists in a sap exuded from lacquer trees of the *Toxicodendron succedaneum (L) Kuntze* species, where the principal component is laccol (C17 unsaturated hydrocarbon chain at the 3-position of the catechol ring). In some part of southern China, *Toxicodendron succedaneum* has also been reported as lacquer sap origins (e.g., in the Guangxi province that is close to Vietnam) (Wan et al., 2007; Heginbotham et al., 2016). Myanmar, Laos, Cambodia, and Thailand lacquers consist of a sap exuded from *Gluta usitata (Wall.) Ding Hou* lacquer tree species, and their principal component is thitsiol (4- and/or 3-substituted catechol derivatives with 17 carbon chains) (Ma et al., 2014). The polyhydroxy phenols (urushiol, laccol, thitsiol) are the main compositions of lacquer and their chemical differences can be intentionally used to differentiate the origin of lacquer sample.

As a cross-linked polymer, Lacquer film is insoluble in most solvents and only a few analytical techniques are appropriate for its analysis. Pyrolysis-gas chromatography/mass spectrometry (Py-GC/MS) is effective and mostly used for lacquer film analysis due to its minimum quantity required, easy sample preparation and effective in lacquer origin tracing. Typical pyrolysis products issued from lacquer samples are principally alkanes, alkenes, alkylbenzenes, alkylphenols and alkylcatechols products (Lu et al., 2012 and references cited therein). If different patterns in the resulting chromatograms can be observed depending on the pyrolysis system used for lacquer analysis (Le Hô et al., 2012), basically, these products are still present and represent the usual markers of origin for the characterization of lacquer samples (Ma et al., 2014). Consequently, by using an extracted ion chromatogram procedure for the treatment of mass spectrometry data, it is possible to identify the components of the lacquer saps to determine the origin of the lacquer samples.

Although lacquer has a long history in China (Zhai et al., 2021) and some researches have disclosed on the ancient lacquer in other areas in China (Jin et al., 2012; Wei et

al., 2011; Jin et al., 2017; Hao et al., 2017; Fu et al., 2020; Zheng et al., 2020; Xiao et al., 2020), there is no specific research dedicated to the lacquer craft of marginal area (e.g., the *Ba* State in the southwest part of China). Furthermore, the beneficial of GCxGC/MS separation of complex additives in lacquer crafting has not yet been explored in archaeological samples except our previous work on pure modern lacquer film (Okamoto et al., 2018).

Ba group was an ethnic group living in southwest China, upper stream of the Yangtze River during a period extending from the Shang Dynasty to the Qin Dynasty (ca.1600 BC-221 BC). The associated *Ba* State developed a stronger power in the Spring and Autumn period (770-476 BC) which continued during the Warring States (476-221 BC). *Ba* State had close cultural and economic exchanges as well as military conflicts with its neighboring *Chu* State (Bai, 2020). Some typical sites of *Ba* culture in the Chongqing area such as the Shuangyantang site in Wushan, the Lijiaba site in Yunyang (Fan and Freestone, 2017), the Yujiaba site in Kai county (Fan et al, 2020), and the Xiaotianxi site in Fuling were unearthed through archaeological discoveries. Among them, the Lijiaba site (Fig.1), located on the eastern bank of the Pengxi river (a branch of the Yangtze River) is known as the regional center of *Ba* state in the Pengxi river basin. Lijiaba site is of utmost importance for the research of *Ba* culture as well as for the findings of evidence of exchanges of these *Ba* people with other cultures that are contemporary to its development.

Figure 1

In order to increase our knowledge on the lacquer crafts of the *Ba* ethnic group, the lacquer film sample from the scabbard of a bronze sword (03YLM11:10) dated to the Warring States period were studied by a multidisciplinary approach including microscopy, scanning electron microscopy-energy dispersive X-ray spectrometers (SEM-EDS), Raman spectroscopy, pyrolysis coupled to gas chromatography/mass spectrometry (Py-GC/MS) and coupled to comprehensive two-dimensional gas chromatography/mass spectrometry (Py-GCxGC/MS). As a result, new elements for a complete description of the lacquer coating of this representative artifact of the *Ba* ethnic group were obtained.

2. Experimental

2.1 The archaeological background and materials

The Lijiaba site is situated in the Qingshu village (Yunyang county), Chongqing, southwest China (31°6′15″N, 108°41′E) (Fig.1). It was discovered in 1987 and archaeological survey and tentative excavations were carried out between 1992 and 1995, prior to regular excavations started in 1997. The collected material remains from this site suggested that it was inhabited during a long period spanning from the Shang-Zhou Dynasty to the Six Dynasties (ca.1600 BC–ca.600 AD) (Chongqing 2001, 2003). The exceptional nature of the findings conducted in the selection of the site as one of the *Top Ten Archaeological Discoveries in China*. Numerous tombs from the Eastern Zhou Dynasty (770-221 BC), which includes the Spring and Autumn period and the Warring States period were excavated there.

Figure 2

Besides bronze (Fan and Freestone 2017) and pottery artefacts (Wu et al. 2013), lacquer film marks and lacquer objects were also found in Lijiaba site (Chongqing. 2001, 2003). The lacquer film residue studied in this paper was found on the scabbard of the bronze sword in the tomb 2003YLM11 (archaeological number 03YLM11:10, Fig.2). The tomb was located in the center of area Ⅲ of Lijiaba site which is a rectangular earthen pit tomb and filled with a lot of green paste mud (Fig.2). Other archaeological objects unearthed with the bronze sword consist in ceramic and bronze artifacts shown in Fig.2.

Figure 3

A relatively small surface of lacquer coating was preserved intact on the surface of the scabbard of the bronze sword. Some small lacquer fragments spontaneously detached from the scabbard were chosen for analysis since they provided lacquer samples of interest in avoiding further sampling, which could be prejudicial for the integrity of the scabbard, already noticeably damaged.

2.2 Microscope observation

Digital microscopy (VHX-5000 Keyence) used in reflection mode permitted to reveal the surface profiles of lacquer samples. The lacquer sample was mounted in epoxy resin at room temperature and polished. And the sample was coated with carbon for SEM analysis. A FEI-Quanta 200 environmental scanning electron microscope (SEM) equipped with an X-ray energy dispersive spectroscopy (EDS) system was utilized to observe morphologies of the samples in high-vacuum mode applying an accelerating voltage of approximately 20 kV.

2.3 Raman spectroscopy

Raman spectra of the sample were recorded at room temperature with a Renishaw inVia Raman microscope system from 3500 to 50 cm^{-1} in extensive mode with a laser wavelength of 532 nm and 50L× objective lens. Laser power was set for emission at 1 percent power, which corresponds to ca. 0.5 mW with an integration time of 10 s. The number of accumulations was fixed from 1 to 10.

2.4 Py-GC/MS Analysis

The Py-GC/MS system consisted of a vertical micro-furnace pyrolyzer PY-2020iD (Frontier Lab, Fukushima, Japan) fitted to a Shimadzu QP2010Plus GC/MS instrument (Shimadzu, Champs-sur-Marne, France). The mass of samples used for analysis lies between 100-130 μg. The samples investigated by Py-GC/MS were cut with a scalpel in tiny pieces after a cleaning and polishing step to eliminate dusts and trace of soil contaminants under binocular magnifier. The state of the archaeological samples permits with difficulty to separate properly the layers of lacquer. Consequently, analysis was conducted on samples presenting the whole stratigraphy of the lacquer's coatings, namely the layers described in section 3.1 below.

The conditions of analysis have been described elsewhere (Avataneo and Sablier, 2017). Briefly, the sample was introduced into the micro-furnace at 500°C; chromatographic separation was conducted on an apolar fused silica capillary column 5% phenyl–95% dimethyl polysiloxane (30 m length, 0.25 mm inner diameter, 0.25 μm film thickness) with a the following oven temperature program: 2 min at 40 °C, ramping at 12 °C min^{-1} to 325 °C, plateau at 325°C for 10 min. The same experimental conditions were applied for thermally-assisted hydrolysis and methylation (THM) Py-GC/MS (Challinor, 2001). Only a volume of 3-5 μL of tetramethyl ammonium hydroxide (25% in methanol) was added to the sample in the sample cup before its introduction in the micro-furnace. The scan range of the mass spectrometer was set from 40 to 500 u, operated at 5000 u. s^{-1}, and ionization was performed by electron ionization at 70 eV. Identification of pyrolysis products was obtained by comparison of their mass spectra with mass spectra of the NIST library (NIST, 2011) and by interpreting the main fragmentations observed.

2.5 Py-GCxGC/MS Analysis

The Py-GCxGC/MS system consisted of a vertical microfurnace pyrolyzer PY-3030D (Frontier Lab, Fukushima, Japan) fitted to a Shimadzu QP2010-Ultra mass spectrometer (Shimadzu, Champs-sur-Marne, France) equipped with a two-stage thermal modulator ZX 2 (Zoex, Houston, TX, USA). Quantities of lacquer sample analyzed were about 50 μg, weighed with a microbalance (XP2U Ultra Micro Balance, Mettler Toledo, Viroflay, France).

The GCxGC chromatography system consisted in an apolar capillary column OPTIMA-5HT (30 m × 0.25 mm I.D., 0.25 μm film thickness, Macherey-Nagel, Hoerdt, France) in the first-dimension, and a moderate polar column Zebron ZB-50 (2.8 m × 0.1 mm I.D., 0.1 μm film thickness, Phenomenex, Le Pecq, France) in the second-dimension and for the loop modulator system. The separation was carried out in a constant pressure mode (300 kPa). The ZX 2 two-stage thermal modulator operated a cooled air jet at −94°C, modulated with a pulsed hot air jet at a modulation period of 9 s, and a programmed hot pulse duration of 0.350 s. Details for the analysis have been reported previously (Okamoto et al, 2018), and consists briefly of an oven temperature program initially held 5 min at 70°C, and increased at 3°C/min to 300°C, where it is held during 20 min. The mass spectrometer was operated at 20,000 $u.s^{-1}$, with a scan range from 45 to 600 u, using electron ionization at 70 eV. Data processing of the Py-GCxGC/MS raw data was achieved using a GC Image software, version 2.4 (Lincoln, NE). As noted above, lacquer components were identified by comparison of their mass spectra with mass spectra of the NIST library (NIST, 2011) and by interpretation of the main fragmentations.

3. Results

3.1. Microscopic observation

Two lacquer film layers, ticked as the first lacquer layer and the second lacquer layer on the ground layer, can be clearly observed (Fig.4A). The first layer is on the top of the ground layer and the second layer is on the top of the first layer. The micrographs of the lacquer base, the first lacquer layer and the second lacquer layer are separately shown in Fig.4B, Fig.4C and Fig.4D, respectively. There are some white, yellow and red particles, as well as some cracks visible on the ground layer in Fig.4B. Similarly, there are some small white and red particles visible on the first lacquer film layer in Fig.4C. Moreover, big particles on the cracks were observed on the second lacquer layer in Fig.4D.

On observation of the whole sample cross-section, the layout of the lacquer sample can be divided into three parts, a lacquer coating divisible in two parts (with a total thickness of ca. 45 μm), a ground layer which is about 360-380 μm thick, and the wood support as shown in Fig.4E. Depending on the angle of view, the layout of the lacquer film layers can be difficult to observe as revealed on the cross-section micrograph in Fig.4F. Large (300 μm*170 μm) and small (20 μm * 50 μm) white or white-yellow particles can be found on the ground layer (Fig.4G and Fig.4H) . Additionally, some holes can also be observed in the ground layer (Fig.4H).

Figure 4

The SEM-EDS results from the analysis of the different layers showed in Fig.5 are depicted in Table 1. The main elements contained in the lacquer sample are carbon (C), oxygen (O), iron (Fe), copper (Cu), lead (Pb), calcium (Ca), phosphorous (P), magnesium (Mg), aluminium (Al) and silicon (Si). The content of calcium and phosphorus in the ground layer is obviously higher than those observed in the lacquer film layers. As reported in Fig.5B-C, distribution patterns for calcium and phosphorus present a similar appearance. Combined with the Raman spectroscopy analysis results (see below in section 3.2), the areas of calcium and phosphorus distribution are nicely correlated to the presence of hydroxyapatite. The copper and lead distributed on the cross-section may likely come from the bronze sword, whereas the silicon present may likely come from the soil.

Figure 5

3.2. Raman spectroscopy analysis

Lacquer sample cross-section was investigated by Raman spectroscopy. The corresponding Raman spectra of the large white or yellow-white particles in the sample and Raman spectra of the hydroxylapatite reference ore ($Ca_{5.00}$ ($P_{1.00}$ $O_4)_3((OH)_{0.98}$ $Cl_{0.02}$)) ('Hydroxylapatite R060180') were shown in Fig.6. The observed Raman peaks at 431, 579, 591, 609, 962, 1047, 1069 and 3574 cm^{-1} are ascribed to the Raman peaks of hydroxyapatite (Timchenko et al, 2018). Small hydroxyapatite particles are observed in the lacquer samples. The small particles are less than 10 μm in size while the larger particles are more than 300 μm in size. This may agree with the use of different particle size of bone powders in different steps of lacquering craft in ground layer formation (e.g., first applying large size particles to fill large holes in the wooden base and then applying small size particles to smooth the surface), a phenomenon previously observed in adjoining *Chu* state lacquerware (Jin et al. 2017; Jin et al. 2012). Cuprite (Cu_2O), anatase (TiO_2) and carbon (amorphous) are also detected on the cross-section in which the origin of cuprite was attributed to the bronze sword while the origin of anatase was attributed to the soil present in the buried environment (Fig.S1, supplementary material).

Figure 6

The detection of the white particles of indeterminate forms is in accordance with the use of powdered bone as a ground layer demonstrated by the cross-sectional views of the lacquer coating in the archaeological sample. The detection of Ca during the SEM-EDX analysis (Fig.5B) confirms this statement. Detection of hydroxyapatite by

Raman spectroscopy also acts in favor of a presence of added crushed bones particles, which is unexpected at first glance and reveals a piece of interesting information on the basic technique of the *Ba* group for the preparation of elemental consolidation layer.

3.3 Py-GC/MS analysis of lacquer origin

The extracted ion chromatograms (EICs) at m/z 91, 107, 108, 123, 124 are reported beside the total ion chromatogram (TIC) in Fig.S2, supplementary material. Table 2 resumes the assignments of the detected pyrolysis products. The fragment ion at m/z 91, chosen for the characterization of alkylbenzenes, showed a distribution of homologues with a predominant alky chain of C1 to C9. The characteristic fragment ions at m/z 107-108 for phenol species, yielded a larger distribution spanning from C5 to C10 in the low homologue region, and peaks attributed to the pentadecenyl and pentadecyl phenols C15 for elution times between 21-23 min (Fig.S2, supplementary material). The m/z 107 fragment corresponds to a direct α C-C bond cleavage on the substituted alkyl chain, and the m/z 108 fragment is issued from a retro-ene rearrangement implying a hydrogen atom on the alkyl chain (Bouchoux et al., 2012). Interestingly, one can notice that the ortho isomers (m/z 107) generally dominate the meta isomers (m/z 108) in the distribution of alkylphenols observed in the corresponding EICs. The meta isomers (m/z 108) were barely observed while the complete series of ortho isomers C5-C12 and the 2-pentadecylphenol markers, $C_{21}H_{36}O$ were observed in the sample analyzed under direct Py-GC/MS conditions (Fig.S2, supplementary material). In comparison, catechol compounds (m/z 123, 124) were barely extracted from the background signal in the chromatograms.

Analysis of the lacquer sample was also conducted under THM pyrolysis conditions. Globally, THM-Py-GC/MS experiments gave concordant results to those reported by Py-GC/MS. In accordance to Py-GC/MS results, the two characteristic catechol markers 1,2-dimethoxy-pentadecylbenzene ($C_{23}H_{40}O_2$, t_r=22.57 min) and 1,2-dimethoxy-pentadecenylbenzene ($C_{23}H_{38}O_2$, t_r=22.45 min) were both detected in the tested sample confirming the *Shengqi* origin. Noteworthy, under THM pyrolysis conditions, kumanotanic acid, mazzeic acid and miyakoshic acid were detected at a low ratio and their presence could be correlated to an ageing process of the urushi sample in particular in presence of siccative oil as reported previously (Schilling et al. 2016; Webb, Schilling, Chang 2016, Tamburini et al. 2016). In comparison to direct Py-GC/MS analysis, the observed alkylbenzene series in the lacquer sample is reduced: only the n-hexylbenzene was present while n-heptylbenzene and n-octylbenzene were only detected at traces level. The distribution of catechols, as reported in the EICs at m/z 151 and 152 (Fig.7), showed a large distribution with

additional catechol markers of lower side-chain length (C4-C5). The distribution of fragment ions at m/z 151 and 152 was observed to extend to the pentadecenyl and pentadecyl catechol C15 homologues for elution times of between 22 and 23 min, as expected for a *Toxicodendron vernicifluum* sap origin (Fig.7, Table 3).

Figure 7

THM-Py-GC/MS permitted to refine the analytical information gained on the sample, noticeably with the characterization of several fatty acid methyl esters. TIC and EICs at m/z 74, characteristic fragment ions for the fatty acid methyl esters, at m/z 151 and 152, characteristic fragment ions for the methylated catechols are reported in Fig.7. Table 3 reports the assignments of these marker ions. In fact, distribution of fatty acid methyl esters was observed with a noticeable high ratio for the peaks associated to palmitic and stearic methyl esters (Fig.7). As well the repartition of the lower components of fatty acid methyl esters (C6-C10) showed a maximum for the C8 homologue (Table 3, t_r=9.71 min). The nonanedioic acid, dimethyl ester, also reported as the dimethyl ester of the azelaic acid ($C_{11}H_{20}O_4$ t_r = 14.57 min), was detected in association with the octanedioic acid, dimethyl ester ($C_{10}H_{18}O_4$ t_r = 13.59 min) and the decanedioic acid, dimethyl ester ($C_{12}H_{22}O_4$ t_r = 15.60 min) (Fig.7, Table 3). The relative proportion of azelaic acid and di-acids of longer chain as well as the presence of palmitic acid were in accordance with the previous detection of those compounds in aged mixtures of urushiol lacquer and drying oil (Tamburini et al., 2016).

3.4 Py-GCxGC/MS analysis of the lacquer sample

Due to the intrinsic grouping features of GCxGC separation (Han et al., 2018), different series of compounds can be easily separated on the resulting Py-GGxGC/MS chromatogram (Fig.8). Among the structures observed, the patterns of typical lacquer component can be observed in the 2D chromatogram with a higher sensitivity and dynamics compared to direct Py-GC/MS: (i) a series of alkane ranging from C10 to C29; (ii) a series of alkene ranging from C10 to C18; (iii) a series of alkylbenzene homologues ranging from C1 to C15; (iv) a series of catechols ranging from C1 to C15. These four series in the Py-GCxGC/MS TIC chromatogram confirmed distinctly the presence of a lacquer originating from *Toxicodendron vernicifluum*. Moreover, as can be seen in the 2D chromatogram, other compounds could be patently highlighted: (i) a series of PAH compounds, which cannot be obtained during classical 1D analysis, (ii) a series of 2-ketones and 7-ketones, similarly difficult to detect by Py-GC/MS, and (iii) other organics (methylphenones, cycloalkenes, furanones) not characterized otherwise.

Figure 8

As stated above, EICs of the m/z 107-108 (characteristic fragments for the alkylphenols) confirmed the *shengqi* origin of the sample in particular with the detection of the characteristic C15 ortho/meta homologues. All the homologues already detected during direct Py-GC/MS were detected here but with an improved characterization of the lower homologues C1-C5, which were hardly extracted from the TIC background during 1D analysis. Moreover, the GCxGC separation conducted to a better detailed picture of positional isomer distribution of alkylphenol markers with the clear differentiation of ortho and meta isomers still observable in a deteriorated archaeological sample, thanks to the sensitivity of the GCxGC separation (Fig.S3, Supplementary materials). Showing a decreasing intensity, the C8-C14 homologues provided the meta isomers for all this group while the ortho isomers were slowly disappearing in the series for homologues above C9. Compare to Py-GC/MS analysis, the complete series of alkylphenols from C1-C15 can be followed in the EIC of m/z 107-108 ion markers of the alkylphenols. Similarly, the EICs for m/z 91 and 92 yielded the complete series of alkylbenzene from the C1 to C15 homologues. Comparatively, as shown above, Py-GC/MS provided an alkylbenzene series from C1 to C11 and no detection of the characteristic C15 homologue. In addition, the lower homologues of the alkylbenzene series are observable with their different positional isomers. Noticeably, the C13 and C14 homologues were visible here and detected at trace level.

EICs for the m/z 55-57 provided a longer distribution of the series of alkanes/alkenes than previously observed during Py-GC/MS analysis since this series was limited to the C15 homologue in 1D analysis. Here, the series of alkanes span from C10 to C29, and alkenes from C10 to C18. Interestingly, if the previous pattern observed during Py-GC/MS analysis with major peaks at C14, C15 are conserved, Py-GCxGC/MS yielded an increased distribution of these major homologues until the C17 homologue for both alkanes and alkenes. Previous results obtained with reference lacquer films provided a similar pattern with the presence of alkanes and alkenes for the C14-C17 homologues in the case of the *Toxicodendron vernicifluum* lacquer sap differentiating it from other lacquer saps (Okamoto et al., 2018). Noticeably, a series of compounds was observed in the previous EIC m/z 91 for which their appearance was improved by the extraction of the base peak at m/z 119 in the chromatogram. Dispersedly distributed around 21-22 min (dimension 1) and ca. 5s (dimension 2), and mixed to the alkylphenol homologues distribution, these compounds were assigned to substituted methylphenyl, ethanone.

Another series of ketone compounds associated to linear structures were observed between 5-62 min (dimension 1) and 3-4s (dimension 2). This series started with the lower homologue: 2-hexanone ($C_6H_{12}O$ MW 100) 5.7 min 2.96 s and continued by incrementation in the number of carbons until the C18 homologue, 2-octadecanone. Besides, a series of alkyl ketones assigned to alkyl, 7-one was observed from C11-C17. From C10 to C12, unsaturated ketones were observed near their associated 2-ketones. Indeed, their detection could not be easily conducted from Py-GC/MS chromatogram as these compounds are noticeably diluted in the global TIC. The fact is that, after observation of this long-chain ketone series in 2D experiments, a backward EIC procedure at m/z 58 for the 1D experiment could only provide a limited part of these series of ketones present in the archaeological lacquer sample, and definitely not their complete distribution revealed in the Py-GCxGC/MS analysis. The observed series of ketones (n-alkan-2-ones) may result from the oxidative burning of vegetation wax alkanes (Simoneit, 2002) as well as from the incomplete combustion of aliphatic compounds (Oros and Simoneit, 2001a). Similarly, α,ω-alkanedioic acids may result from the oxidation of biopolymers, of other lipid compounds (e.g. ω-hydroxyalkanoic acids), or from the incomplete combustion of other products. In particular, the presence of α,ω-nonanedioic acid was previously rationalized through the potential photooxidation of C18:1 and C18:2 alkenoic acids (Oros and Simoneit, 2001b). Nevertheless, no any trace of unsaturated fatty acids was detected during our investigations.

PAH compounds such as naphthalene, fluorene, anthracene, phenanthrene, and pyrene can be well separated and detected together with their methylated homologues (Fig.8) (Table S1 Supplementary Materials). However, no markers of presence for PAH derived compounds were characterized during the above direct Py-GC/MS analysis (Table 2 and 3). The lack of detection of PAHs during 1D analysis can be rationalized by the complexity of the components resulting in a mixture hardly resolved by a one dimension GC/MS analysis. As a consequence, the detection and characterization of PAHs that can hardly be fully characterized by 1D analysis constitutes one of the most interesting improvement provided here by the use of the GCxGC separation.

4. Discussion

4.1 Bone-derived ground layer of *Ba* lacquering

Bone-derived ground layer (骨粉打底) has a long tradition in ancient Chinese lacquering. Scholars have speculated that this tradition was early used in Han dynasty

(202BC-220AD) which was testified by scientific analysis of Han lacquerwares (Jin, 2008). Later, the discovery of bone-derived ground layer from lacquerware in Jiuliandun tomb (*Chu* state) traced this tradition back to the Warring States (Jin et al., 2017). The discovery of bone-derived ground layer on *Ba* state testified the previous observation of Dr. Jin in lacquer wares from the Warring States period (Jin et al., 2012; Jin et al., 2017). The analytical evidence supports that different size particles of hydroxyapatite from bone was added to the lacquer base during its making process, confirming the old recorded recipes of lacquer coating making in ancient China (Jin et al., 2017) and the earliest one of *Ba* state.

These particles of hydroxyapatite appeared to be added to the ground layer without presenting a regular and reproducible size pattern in the process of lacquer making: this observation agrees with the use of different particle size of bone powders in different steps of lacquering craft in ground layer formation, a phenomenon previously observed in adjoining Chu state lacquerware (Jin et al., 2017; Jin et al., 2012). Due to the cracks, the application steps of different size bone particles cannot be clearly differentiated in the tested samples. The same traditions found in *Ba* state and *Chu* state showed evident similarity in the lacquering, inferring the cultural and craft communications between these two adjoining states. In addition, ground layer with other composition or no ground layer (Wei et al., 2011; Fu et al., 2020) has also been reported which showed diversified lacquer crafting during the Warring States. Down from this period, this tradition has a long and wide use that can be often found in old Korean lacquerware and Chinese old lacquerware while the Japanese lacquerware doesn't show such powdered bone foundation (Urushi 1988; Hao et al, 2021).

4.2 Lacquer sap and drying oil in *Ba* lacquerware

If the use of drying oil like tung oil has been previously characterized in Japanese export lacquer from modern time (Heginbotham and Schilling, 2011), the use of tung oil has been mostly documented in Chinese lacquer (Hao et al., 2019; Tamburini et al., 2015) and the concomitant detection of oil and lacquer mixture in archaeological samples is always a matter of interest to increase our knowledge on lacquer fabrication. In previous experiments associating urushi lacquer and tung oil as a mixture, a relatively low abundance of azelaic acid was reported and its low abundance was correlated to the presence of induced cross-linking at a higher degree when the oil was added to urushi (Tamburini et al. 2016). Additionally, during the same experiments, the proportion of short chain fatty acids was observed to increase. Noticeably, under the THM pyrolysis conditions applied here, numerous fatty acids

C6-C10 were observed (Table 3), an observation in accordance with the addition of drying oil in the sample. In the absence of any other contradiction, assumption of the use of tung oil can be considered in view of its previous detection in Asian lacquer (Hao et al., 2019; Tamburini et al. 2015).

The presence of drying oil was observed previously in ancient samples dated from the Jōmon period in Japan, suggesting that the mastered technic of mixing lacquer sap with dry oil in the purpose of increasing luster and elastic of lacquer film was early employed in the premise of lacquer making technique (Yuasa et al., 2015). Drying oils have also been characterized recently in Chinese lacquer samples of the Warring States period (Fu et al., 2020) and even, feasibility studies have been attempted to quantify drying oil in ancient lacquerwares using FTIR spectroscopy (Xiao et al., 2020). The detection of markers of potential drying oil addition in the sample of the *Ba* ethnic group is in accordance with these experiments. The formation of azelaic acid, as well as the formation of other similar dicarboxylic acids rationalized by oxidation processes of polyunsaturated fatty acids, can be proposed as a manifestation of an autoxidation phenomenon of drying oils present in the sample (Tamburini et al., 2016). However, the possibility that formation of these dicarboxylic acids results from the oxidation of soot components cannot be completely ruled out, at the present state of investigations, and must be kept as an assumption (Oros and Simmoneit, 2001a, 2001b).

4.3 Soot additives revealed by GCxGC separation

As reported in the table of assignment of PAH related homologues (Table S1, Supplementary materials), we observed more easily the presence of methylphenanthrenes and dimethylphenanthrenes than the same homologues for anthracene, methyl- and dimethylanthracenes in the lacquer sample. A lower abundance of alkylanthracenes compared to alkylphenanthrenes in sedimentary rocks is proposed to account for a widespread terpenoid origin to explain the presence of alkylphenanthrenes (Smith et al., 1995): this fact correlates well with the use of plant soot as black carbon source in the elemental consolidation lacquer layer of the wooden scabbard. Indeed, the absence of structures commonly related to pyrolytic PAHs like benzo[e]pyrene, benzo[a]pyrene, benzofluoranthenes, is in accordance with the soot origin of the detected PAH homologues acting as a coloring material in the fabrication of lacquer artifacts belonging to the Warring States period.

However, assignment of the origin of PAHs in archaeological remains a matter of discussion and shows difficulties in defining attribution of originating processes (Zou et al., 2010). The absence of terpenic markers could act in the use of other species

than softwood species (e.g., pines, spruces, larches). In particular, retene, a well-known marker of abietic acid degradation was absent, which casts doubt on the use of pine wood species (Ren et al., 2018; Karp et al., 2020). Conversely, if the detection of an enlarged series of alkane homologues by Py-GCxGC/MS could be correlated with combustion processes of pine wood species, specificity of theses alkanes/alkenes as wood markers is questionable (Simoneit, 2002). More interestingly, the presence of the mono-, di-, tri-methylated PAHs (naphthalene, anthracene, pyrene) may be correlated to the use of a wood species with bark as material for soot making (Achten et al., 2015).

5. Conclusion

In this paper, composition of the lacquer layers of the scabbard of a bronze sword dating from the Warring States (475-221 BC) and excavated from a *Ba* tomb of the Lijiaba site (Chongqing, southwest China) was investigated. Based on the experimental results obtained in the course of a multidisciplinary approach, the lacquer material constitutive of the decorative coating of the wooden scabbard was assigned to *Shengqi* origin with the characterization of chemical markers of *Toxicodendron vernicifluum* lacquer trees. Additionally, the detection of hydroxyapatite particles and the cartography of chemical elements in the sample are in accordance with the use of crushed bone material in the composition of the ground layer of lacquer. Worthy of mention, Py-GC/MS analysis of the scabbard lacquer sample conducted to the assignment of origin for the lacquer sap and suggested the presence of drying oil addition in relation to the lacquer-making recipes, whilst Py-GCxGC/MS, due to its sensibility and extended resolution, demonstrated unequivocally the presence of other compounds, and particularly PAHs which are attributed to the use of soot of plant origin for coloring of the lacquer.

The present study, which investigated for the first time an archaeological sample of the *Ba* ethnic group of southwest China, permitted to increase our knowledge of the lacquer making crafts of *Ba* state that has been hindered until now due to the rareness of lacquer samples unearthed in ancient *Ba* state locations. Moreover, the present experimental study provides the base for the comparison of lacquer samples coming from adjacent regions and central states upon further study of valuable interest to introduce connection between craft shift, manufacturing techniques and chemical analysis strategies. In light of the present work, future research combining the techniques employed here should permit further investigations of the ancient lacquer

craft in China to refine data and to explore existing relationships between ethnic groups in the sharing of lacquer manufacturing techniques.

Funding: BH thanks to the Fundamental Research Funds for the Central Universities and Postdoctoral Science Foundation for support.

Declarations of interest: none

References

Achten, C., Beer, F.T., Stader, C., Brinkhaus, S.G., 2015. Wood-specific polycyclic aromatic hydrocarbon (PAH) patterns in soot using gas chromatography-atmospheric pressure laser ionization-mass spectrometry (GC-APLI-MS). Environ. Forensics 16, 42-50. https://doi-org.proxy.mnhn.fr/10.1080/15275922.2014.991004.

Heginbotham, A., Chang, J., Khanjian, H., Schilling, M.R., 2016. "Some Observations on the Composition of Chinese Lacquer." Studies in Conservation 61 (sup3): 28-37. https://doi.org/10.1080/00393630.2016.1230979.

Avataneo, C., Sablier, M., 2017. New criteria for the characterization of traditional East Asian papers. Environ. Sci. Pollut. Res. 24(2), 2166-2181. https://doi.org/10.1007/s11356-016-6545-0.

Bai, J., 2020. The Ba culture in the field of archaeometry: conception, problem and method. Yangtze River Civilization, 3, 1-11. (in Chinese).

Bouchoux, G., Sablier, M., Miyakoshi, T., Honda, T., 2012. A 'meta effect' in the fragmentation reactions of ionised alkyl phenols and alkyl anisoles. J. Mass Spectrom. 47, 539-46. https://doi.org/10.1002/jms.2977.

Challinor, J. M., 2001. Review: the development and applications of thermally assisted hydrolysis and methylation reactions. J. Anal. Appl. Pyr. 61, 3-34.

Chongqing, 2001. *Collections of reports on the archaeological excavation in the three Gorges Dam, Chongqing in 1997* (Sciences Press: Beijing).

Chongqing, 2003. *Collections of reports on the archaeological excavation in the three Gorges Dam, Chongqing in 1998* (Sciences Press: Beijing).

Fan, X., Freestone I.C., 2017. Occurrence of phosphatic corrosion products on bronze swords of the Warring States period buried at Lijiaba site in Chongqing, China. Heritage Sci. 5, 48. https://doi.org/10.1186/s40494-017-0161-2.

Fan, X., Wang, Q., Wang, Y., 2020. Non-destructive in situ Raman spectroscopic investigation of corrosion products on the bronze dagger-axes from Yujiaba site in Chongqing, China. Archaeol Anthropol Sci 12, 90. https://doi.org/10.1007/s12520-020-01042-0

Fu, Y., Chen, Z., Zhou, S., Wei, S., 2020. Comparative study of the materials and lacquering techniques of the lacquer objects from Warring States Period China. J. Archaeological Sci. 114, 105060. https://doi.org/10.1016/j.jas.2019.105060.

Han, B., Lob, S., Sablier, M, 2018. Benefit of the Use of GCxGC/MS Profiles for 1D GC/MS Data Treatment Illustrated by the Analysis of Pyrolysis Products from East Asian Handmade Papers. J. Am. Soc. Mass Spectrom. 29, 1582–1593. https://doi.org/10.1007/s13361-018-1953-7

Hao, X., Wu, H., Zhao, Y. et al, 2017. Analysis on the Composition/structure and Lacquering Techniques of the Coffin of Emperor Qianlong Excavated from

the Eastern Imperial Tombs. Sci. Rep. 7, 8446 1-11. https://doi.org/10.1038/s41598-017-08933-8

Hao, X., Schilling, M. R., Wang, X., Khanjian, H., Heginbotham, A., Han, J., Auffret, S., Wu, X., Fang, B., Tong. H. 2019. "Use of THM-PY-GC/MS Technique to Characterize Complex, Multilayered Chinese Lacquer." Journal of Analytical and Applied Pyrolysis 140 (June): 339-48. https://doi.org/10.1016/j.jaap.2019.04.011.

Hao, X., Wang, X., Zhao, Y., Tong, T., Gong, Y., 2021. Identification of minerals and mineral pigments in lacquer by the comprehensive comparative analysis of spectroscopy information, Spectroscopy Letters, 54:6, 446-457, DOI: 10.1080/00387010.2021.1940208

Heginbotham, A., Schilling, M., 2011. New Evidence for the use of Southeast Asian raw materials in seventeenth-century Japanese export lacquer, in: S. Rivers, R. Faulkner, R. Boris Pretzel (Eds.), East Asian Lacquer: Material Culture, Science and Conservation, Archetype Publications, London, pp. 92-106.

Heginbotham, A., Chang, J., Herant, K., Schilling, M.R., 2016. "Some Observations on the Composition of Chinese Lacquer." Studies in Conservation 61 (sup3): 28-37. https://doi.org/10.1080/00393630.2016.1230979.

'Hydroxylapatite R060180'. http://rruff.info/apatite/display=default/R060180.

Jin, P.J., 2008. The Lacquering Technique of Han Dynasty. University of Science and Technology of China.

Jin, P.J., Hu, Y.L., Ke, Z.B., 2017. Characterization of lacquer films from the middle and late Chinese warring states period 476–221BC. Microscopy Res. Techn. 80, 1344-50. https://doi.org/10.1002/jemt.22947.

Jin P.J., Hu Y., Gu X., Ji X., 2012. Research on the Making Techniques about Lacquer Plaster Layer of Lacquer Wares Excavated from Jiuliandun Tombs [J]. Jianghan Archaeology. (in Chinese)

Karp, A.T., Holman, A.I., Hopper, P., Grice, K., Freeman, K.H., 2020. Fire distinguishers: Refined interpretations of polycyclic aromatic hydrocarbons for paleo-applications. Geochimica Cosmochimica Acta 289, 93–113. https://doi.org/10.1016/j.gca.2020.08.024.

Karpova, E., Nefedov, A., Mamatyuk, V., Polosmak, N., Kundo, L., 2017. Multi-analytical approach (SEM-EDS, FTIR, Py-GC/MS) to characterize the lacquer objects from Xiongnu burial complex (Noin-Ula, Mongolia). Microchemical J. 130, 336-44. https://doi.org/10.1016/j.microc.2016.10.013.

Le Hô, A.-S., Regert, M., Marescot, O., Duhamel, C., Langlois, J., Miyakoshi, T., Genty, C., Sablier, M., 2012. Molecular criteria for discriminating museum Asian lacquerware from different vegetal origins by pyrolysis gas chromatography/mass spectrometry. Anal. Chim. Acta 710, 9-16. https://doi.org/10.1016/j.aca.2011.10.024.

Lu, R., Honda, T., Miyakoshi, T., 2012. 'Application of Pyrolysis-Gas Chromatography/Mass Spectrometry to the Analysis of Lacquer Film.' in Dr. Mustafa Ali Mohd (ed.), *Advanced Gas Chromatography-Progress in*

Agricultural, Biomedical and Industrial Applications (InTech Europe 2012, Croatia.).

Ma, X., Lu, R., Miyakoshi, T., 2014. Application of Pyrolysis Gas Chromatography/Mass Spectrometry in Lacquer Research: A Review. Polymers 6, 132-44. https://doi.org/10.3390/polym6010132.

NIST Mass Spec Data Center, S.E. Stein, director (2011) "Mass Spectra" in WebBook of Chemistry, NIST Standard Reference Database Number 69, Eds. P.J. Linstrom and W.G. Mallard, National Institute of Standards and Technology, Gaithersburg MD, 20899, http://webbook.nist.gov

Okamoto, S., Honda, T., Miyakoshi, T., Han, B., Sablier, M., 2018. Application of pyrolysis-comprehensive gas chromatography/mass spectrometry for identification of Asian lacquers. Talanta 189, 315-23. https://doi.org/10.1016/j.talanta.2018.06.079.

Oros, D.R., Simoneit B.R.T., 2001a. Identification and emission factors of molecular tracers in organic aerosols from biomass burning Part 1. Temperate climate conifers. Appl. Geochem. 16, 1513-1544. https://doi.org/10.1016/S0883-2927(01)00021-X.

Oros, D.R., Simoneit B.R.T., 2001b. Identification and emission factors of molecular tracers in organic aerosols from biomass burning Part 2. Deciduous trees. Appl. Geochem. 16, 1545-1565. https://doi.org/10.1016/S0883-2927(01)00022-1.

Ren, M., Wang, R., Yang, Y. 2018. Identification of the proto-inkstone by organic residue analysis: a case study from the Changle Cemetery in China. Herit Sci 6, 19. https://doi.org/10.1186/s40494-018-0184-3

Schilling, M.R., Heginbotham, A., van Keulen, H., Szelewski, M., 2016. Beyond the basics: A systematic approach for comprehensive analysis of organic materials in Asian lacquers. Studies in Conservation 61, 3-27. https://doi.org/10.1080/00393630.2016.1230978.

Simoneit B. R.T., 2002. Biomass burning — a review of organic tracers for smoke from incomplete combustion. Applied Geochem. 17, 129–162. https://doi.org/10.1016/S0883-2927(01)00061-0.

Smith, J. W., George, S. C., Batts, B. D., 1995. The geosynthesis of alkylaromatics. Org. Geochem. 23(1), 71-80. https://doi.org/10.1016/0146-6380(94)00101-6.

Tamburini, D., Bonaduce, I., Colombini, M.P., 2015. Characterization and identification of urushi using in situ Pyrolysis/silylation-Gas Chromatography-Mass Spectrometry. J. Anal. Applied Pyr. 111:33-40 https://doi.org/10.1016/j.jaap.2014.12.018.

Tamburini, D., Sardi, D., Spepi, A., Duce, C., Tinè, M.R., Colombini, M.P., Bonaduce, I., 2016. An investigation into the curing of urushi and tung oil films by thermoanalytical and mass spectrometric techniques. Polymer Degrad. Stability 134, 251-64. https://doi.org/10.1016/j.polymdegradstab.2016.10.015.

Timchenko, P. E., Timchenko, E. V., Pisareva, E. V., Vlasov, M. Y., Volova, L. T., Frolov, O. O., Kalimullina, A. R., 2018. Experimental studies of

hydroxyapatite by Raman spectroscopy. Journal of optical technology, 85(3), 130-135.

Urushi: Proceedings of the 1985 Urushi Study Group, N.S. Brommelle and Perry Smith, editors. 1988 J. Paul Getty Trust.

Wan, Y-Y, Lu R., Du Y-M., Honda T., Miyakoshi T.. 2007. "Does Donglan Lacquer Tree Belong to Rhus Vernicifera Species?" International Journal of Biological Macromolecules 41 (5): 497-503.

Webb, M., Schilling, M.R., Chang, J., 2016. The reproduction of realistic samples of Chinese export lacquer for research. Studies in Conservation 61, 155-65. https://doi.org/10.1080/00393630.2016.1227116.

Wei, S., Pintus, V., Pitthard, V., Schreiner, M., Song, G., 2011. Analytical characterization of lacquer objects excavated from a Chu tomb in China. J. Archaeological Sci. 38, 2667-74. https://doi.org/10.1016/j.jas.2011.05.026.

Wu, Q.Q., Zhu, J.J., Liu, M.T., Zhou, Z., An, Z., Huang, W., He, Y.H., Zhao, D.Y., 2013. PIXE-RBS analysis on potteries unearthed from Lijiaba Site. Nuclear Instruments and Methods in Physics Research Section B: Beam Interactions with Materials and Atoms 296, 1-6. https://doi.org/10.1016/j.nimb.2012.12.004.

Xiao, Q., Wei, S., Fu, Y-C., 2020. Feasibility Study on Quantitative Analysis of Ancient Lacquer Films by Infrared Spectroscopy. Spectroscopy Spectral Analysis 40(9), 2962-2967.

Yuasa, K., Honda, T., Lu, R., Hachiya, T., Miyakoshi, T., 2015. Analysis of Japanese ancient lacquerwares excavated from Jomon period ruins. J. Anal. Appl. Pyr. 113: 73–77. https://doi.org/10.1016/j.jaap.2014.10.018.

Zheng, L., Wang, L., Zhao, X., Yang, J., Zhang, M., Wang, Y., 2020. Characterization of the materials and techniques of a birthday inscribed lacquer plaque of the Qing Dynasty. Heritage Sci. 8(116), 1-10. https://doi.org/10.1186/s40494-020-00462-4.

Zhai, K., Sun, G., Zheng, Y., Wu, M., Zhang, B., Zhu, L., & Hu, Q. (2021). The earliest lacquerwares of China were discovered at Jingtoushan site in the Yangtze River Delta. Archaeometry, 1– 9. https://doi.org/10.1111/arcm.12698

Zou, S., Li, R., Xie, S., Zhu, J., Wang, X., Huang, J., 2010. Paleofire indicated by polycyclic aromatic hydrocarbons in soil of Jinluojia archaeological site, Hubei, China. J. Earth Sci. 21, 247-56. https://doi.org/10.1007/s12583-010-0089-x.

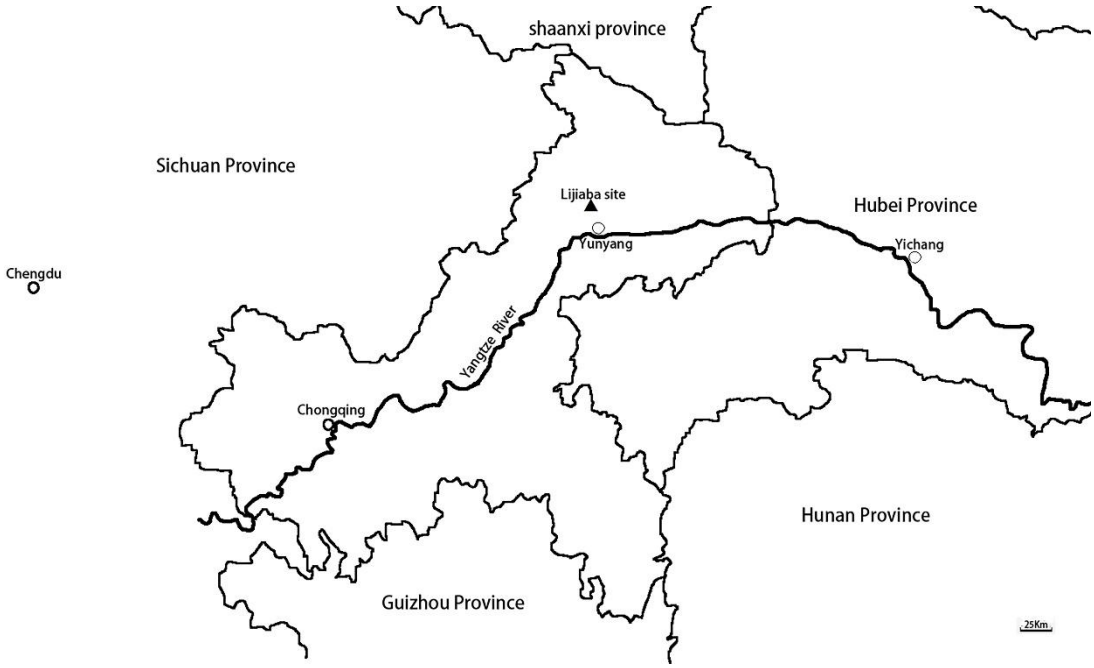

Fig.1. Location map of the Lijiaba site.

672

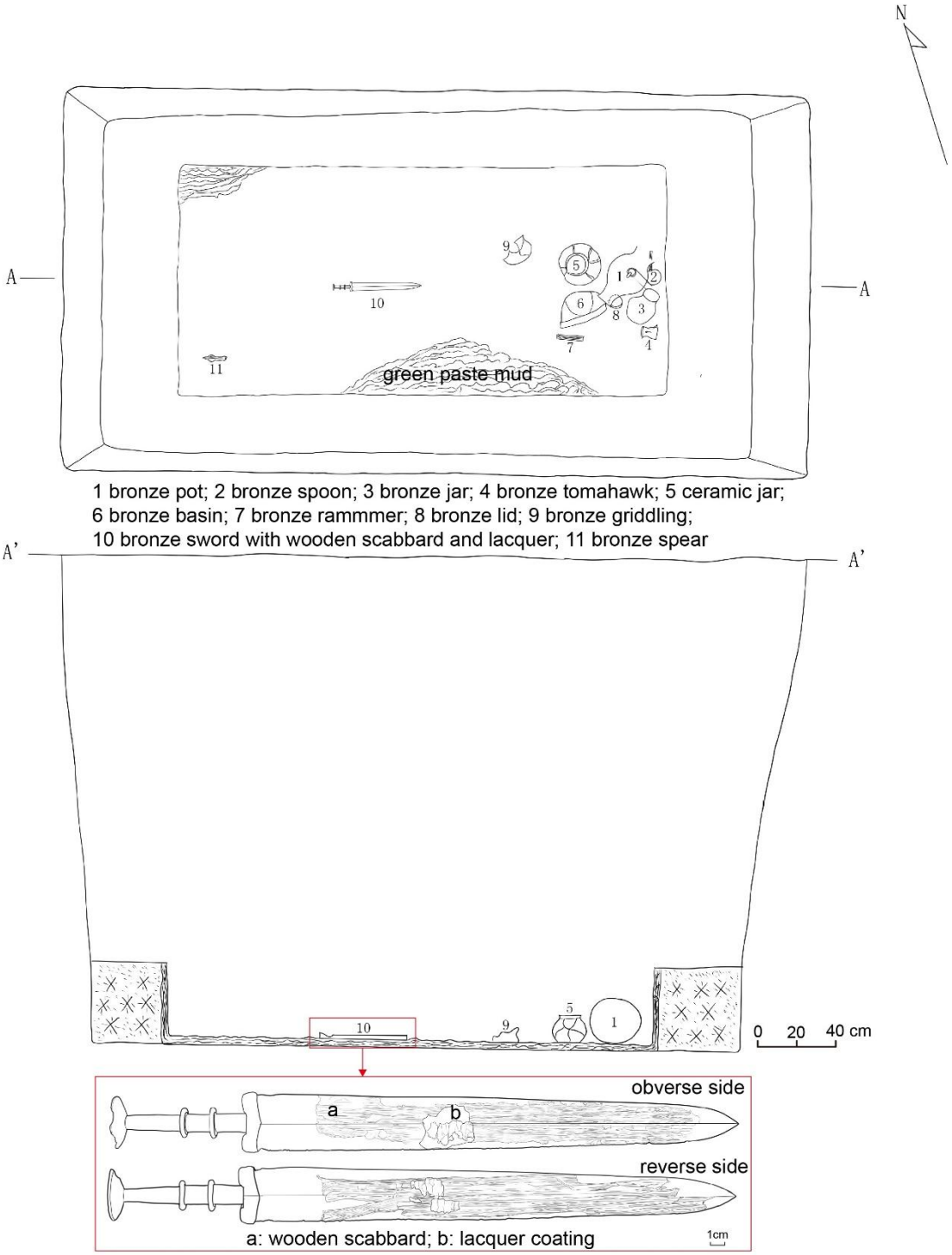

673

674 Fig.2. Plan of the tomb and list of the objects found.

675

676 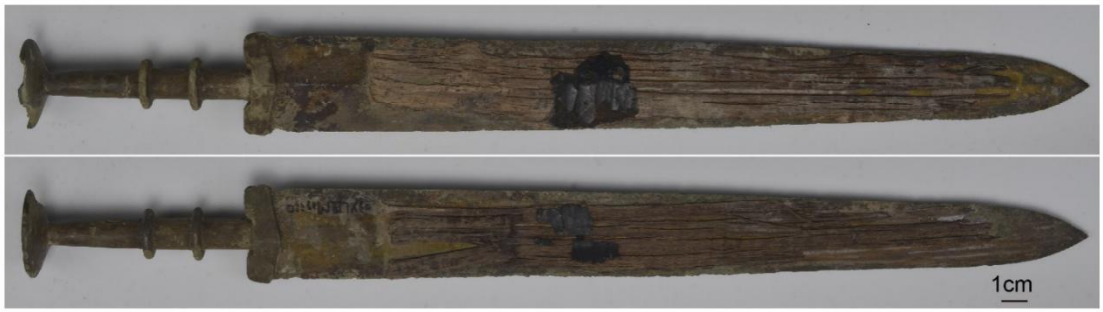

677 Fig.3. Photograph of the bronze sword with its scabbard (archaeological number
678 03YLM11:10).

679

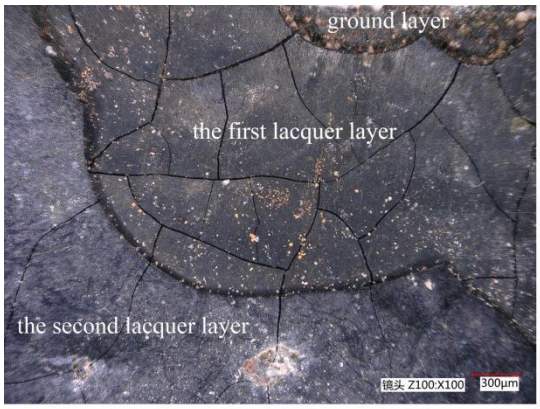

A

B

C

D

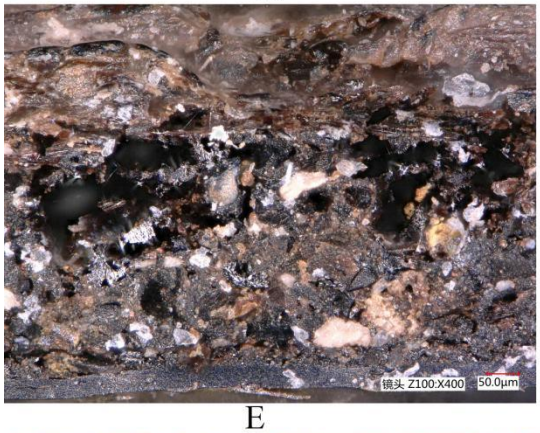

E

F

G

H

680

Fig.4. The surface micrographs of lacquer sample from Lijiaba site: (A) lacquer sample (B) ground layer, (C) the first lacquer layer, (D) the second lacquer layer. Cross-section micrographs of lacquer sample from Lijiaba site: (E) whole lacquer sample cross-section, (F) cross-section of the lacquer film layers, (G, H) cross-section of the ground layer.

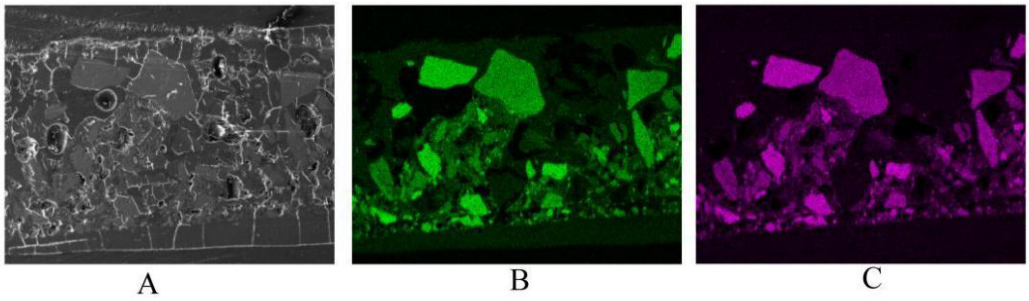

Fig.5. SEM-EDS elemental maps of Ca and P (A) SEM image of the analyzed area, (B) SEM-EDS elemental map of Ca, (C) SEM-EDS elemental map of P.

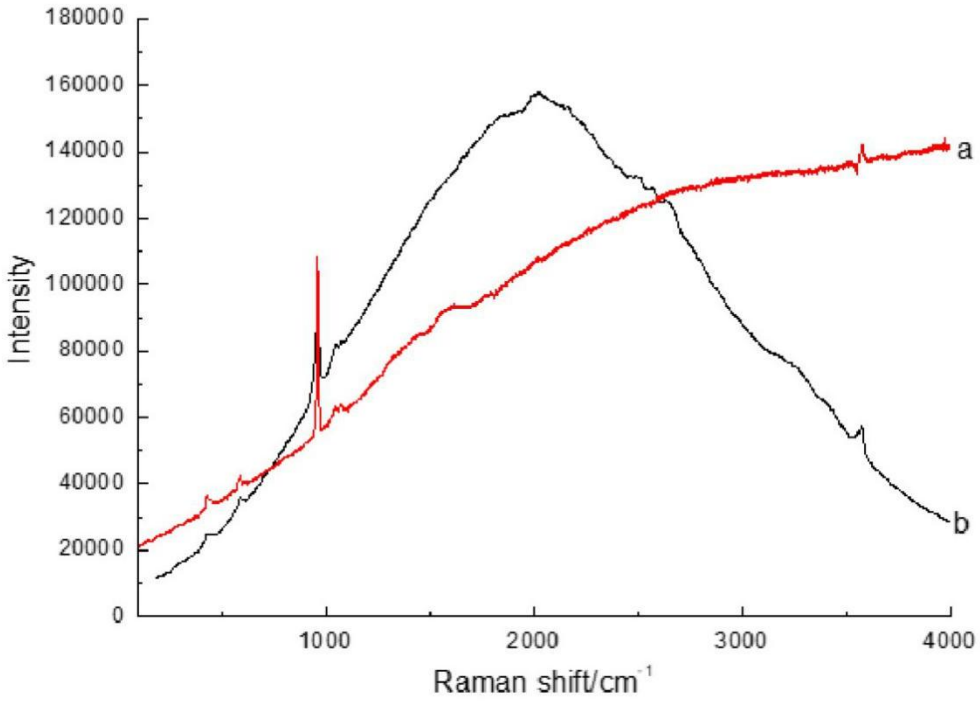

Fig.6 The Raman spectra of the lacquer samples and a standard ore (a: lacquer sample, b: (Ca5.00 (P1.00 O4)3((OH)0.98 Cl0.02))

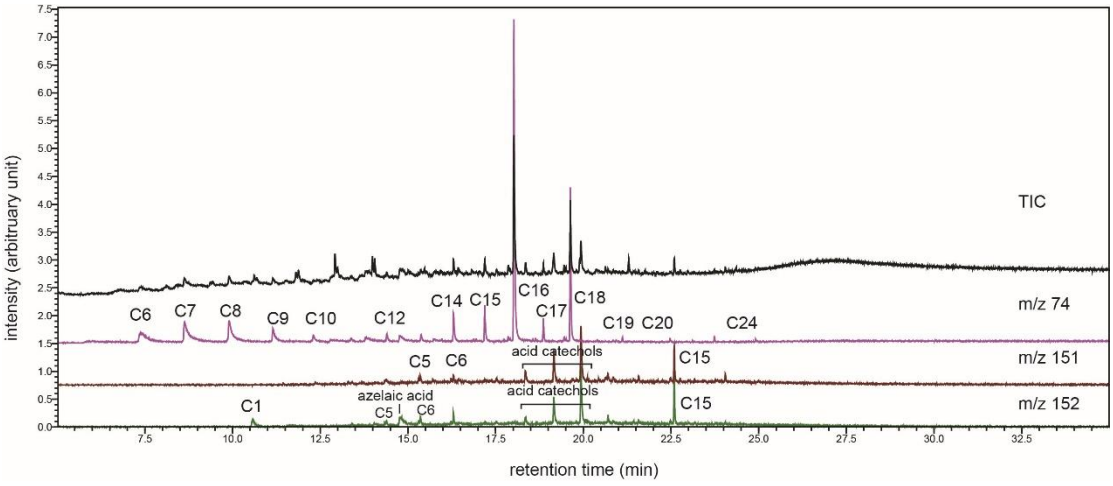

694

695 Fig.7. The chromatograms obtained after pyrolysis of the tested sample under
696 THM-Py-GC/MS where the total ion current (upper trace) and extracted ion
697 chromatograms at m/z 74, 151, 152 are reported (see text for further description).

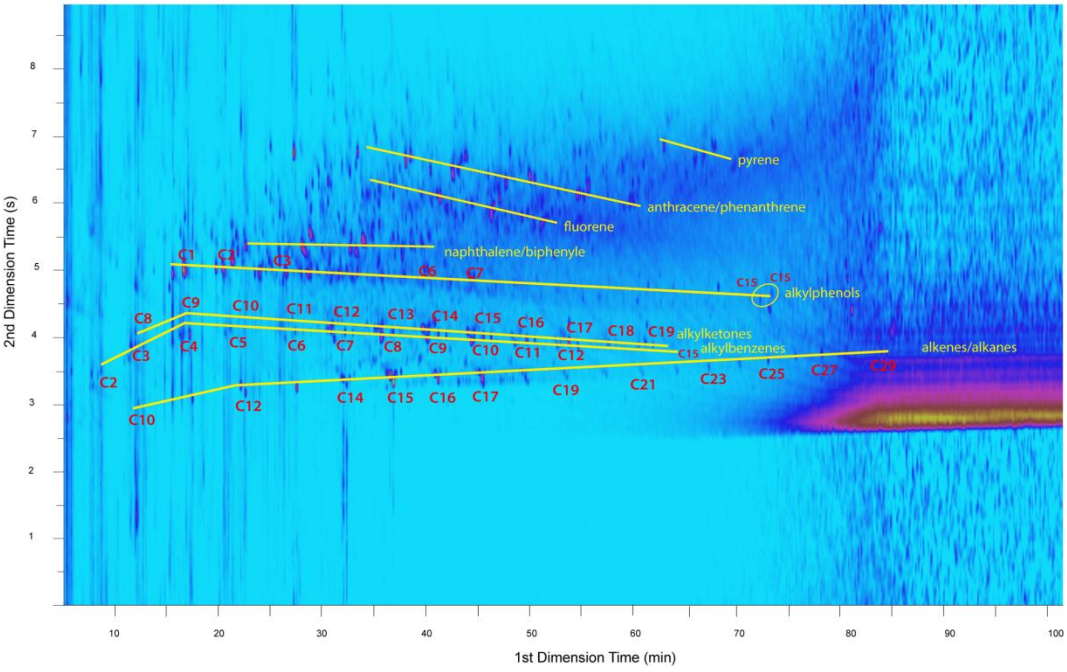

698

699 Fig.8. the 2D chromatograph of the lacquer sample.

700

701

Table 1**.** SEM-EDS results of the lacquer sample analysis

Analysis area		C	O	Fe	Cu	Pb	Ca	P	Mg	Al	Si	S	K
First lacquer film layer	1	44.52	41.11	7.37	2.76	0.05	0.01	0.03	0.28	1.8	2.00	0.03	0.03
	2	48.71	39.26	6.13	2.44	0.09	0.07	0.00	0.18	1.4	1.59	0.05	0.07
	3	58.61	31.46	5.36	3.36	0.04	0.04	0.02	0.21	0.46	0.39	0.05	0.01
Second lacquer film layer	1	46.1	40.02	5.00	3.85	0.4	0.2	0.04	0.29	1.74	2.14	0.08	0.14
	2	34.97	45.53	6.92	2.69	0.24	0.17	0.03	0.51	3.64	4.95	0.06	0.30
Ground layer	1	44.69	35.63	5.76	7.6	0.65	0.84	0.59	0.26	1.63	2.16	0.05	0.14
	2	44.5	36.48	5.62	4.46	0.36	2.05	0.77	0.32	2.14	2.78	0.09	0.43
	3	40.48	27.45	2.09	19.67	1.27	3.87	1.74	0.1	0.56	2.58	0.06	0.13

Table 2. Assignment of the main markers detected by Py-GC/MS in the investigated lacquer sample with retention time (t_r), main fragment ions, expected molecular weights, assigned formula and most likely attribution of the products.

Compounds	t_r (min)	fragment ions (in decreasing order of intensity)	MW	formula	assignement
Alkanes, alkenes					
	3.27	43,41,57,71,56		C_7H_{16}	n-Heptane
	4.85	43,41,85,55,57	114	C_8H_{18}	n-Octane
	6.46	43,57,91,41,85	128	C_9H_{20}	n-Nonane
	7.99	57,43,71,41,70	142	$C_{10}H_{22}$	n-Decane
	9.28	55,69,56,41,70	154	$C_{11}H_{22}$	1-Undecene
	9.36	57,43,41,71,85	156	$C_{11}H_{24}$	n-Undecane
	10.54	55,41,69,43,56	168	$C_{12}H_{24}$	1-Dodecene
	10.64	57,43,41,71,85	170	$C_{12}H_{26}$	n-Dodecane
	11.75	55,43,41,69,56	182	$C_{13}H_{26}$	1-Tridecene
	11.83	57,43,71,85,41	184	$C_{13}H_{28}$	n-Tridecane
	12.88	55,69,43,41,57	196	$C_{14}H_{28}$	1-Tetradecene
	12.96	57,43,71,41,85	198	$C_{14}H_{30}$	n-Tetradecane
	13.96	43,57,55,83,41	210	$C_{15}H_{30}$	1-Pentadecene
	14.04	57,43,71,85,41	212	$C_{15}H_{32}$	n-Pentadecane
alkylbenzenes					
	4.40	91,92,65,63,51	92	C_7H_8	toluene

	6.03	91,106,65,77,51	106	C_8H_{10}	Ethylbenzene
	7.50	91,120,92,65,105	120	C_9H_{12}	n-Propylbenzene
	8.86	91,92,134,115,65	134	$C_{10}H_{14}$	n-Butylbenzene
	10.23	91,92,83,55	148	$C_{11}H_{16}$	n-Pentylbenzene
	11.48	91,92,105,43,162	162	$C_{12}H_{18}$	n-Hexylbenzene
	12.68	92,91, 65,176	176	$C_{13}H_{20}$	n-Heptylbenzene
	13.79	92, 91,43,79,105	190	$C_{14}H_{22}$	n-Octylbenzene
	14.86	92,91,41,55,69	204	$C_{15}H_{24}$	n-Nonylbenzene
alkylphenols					
	13.42	107,108,123,164,77	164	$C_{11}H_{16}O$	2-Pentylphenol ^{t}
	14.46	107,108,155,77,137	178	$C_{12}H_{18}O$	2-Hexylphenol
	15.44	107,108,77,79,192	192	$C_{13}H_{20}O$	2- Heptylphenol
	16.40	107,108,77,119,206	206	$C_{14}H_{22}O$	2-Octylphenol ^{t}
	17.31	107,108,136,220,165	220	$C_{15}H_{24}O$	2-Nonylphenol ^{t}
	22.02	107,108,304,43,94	304	$C_{21}H_{36}O$	2-Pentadecylphenol
Monocarboxylic fatty acid					
	18.33	73, 43,57,60,41	256	$C_{16}H_{32}O_2$	Hexadecanoic acid (palmitic acid) ^{t}
	19.90	73, 43,57,60,55	284	$C_{18}H_{36}O_2$	Octadecanoic acid (stearic acid) ^{t}

* co-elution, superscript ^{t} means that only a trace of compounds was detected

Table 3. Assignment of the main markers detected by THM Py-GC/MS in the investigated lacquer sample with retention time (t_r), main fragment ions, expected molecular weights, assigned formula and most likely attribution of the products.

Compounds	**t_r (min)**	**fragment ions (in decreasing order of intensity)**	**MW**	**formula**	**assignement**
Alkanes, alkenes					
	6.42	43,57,91,41,85	128	C_9H_{20}	n-Nonane
	7.90	41,55,56,43,70	140	$C_{10}H_{20}$	1-Decene
	7.99	57,43,71,41,70	142	$C_{10}H_{22}$	n-Decane
	9.25	55,69,56,41,70	154	$C_{11}H_{22}$	1-Undecene
	9.34	57,43,41,71,85	156	$C_{11}H_{24}$	n-Undecane
	10.53	55,41,69,43,56	168	$C_{12}H_{26}$	1-Dodecene
	10.62	57,43,41,71,85	170	$C_{12}H_{26}$	n-Dodecane
	11.75	55,43,41,69,56	182	$C_{13}H_{26}$	1-Tridecene
	11.82	57,43,71,85,41	184	$C_{13}H_{28}$	n-Tridecane
	12.86	55,69,43,41,57	196	$C_{14}H_{28}$	1-Tetradecene
	12.95	57,43,71,41,85	198	$C_{14}H_{30}$	n-Tetradecane
	13.93	43,57,55,83,41	210	$C_{15}H_{30}$	1-Pentadecene

	14.00	57,43,71,85,41	212	$C_{15}H_{32}$	n-Pentadecane
alkylbenzenes					
	11.45	91,92,65,79,162	162	$C_{12}H_{18}$	n-Hexylbenzene
	12.64	92,91, 65,176	176	$C_{13}H_{20}$	n-Heptylbenzene ᵗ
	13.75	92,55,91,190	190	$C_{14}H_{22}$	n-Octylbenzene* ᵗ
Methyl ester acid catechols					
	18.30	136,151,91,266,152	266	$C_{15}H_{22}O_4$	Methyl-6-(2,3-dimethoxyphenyl)hexanoate (miyamic acid)
	19.10	136,151,152,91,280	280	$C_{16}H_{24}O_4$	Methyl-7-(2,3-dimethoxyphenyl) heptanoate (kumanotanic acid)
	19.89	136,152,151,294,91	294	$C_{17}H_{26}O_4$	Methyl-8-(2,3-dimethoxyphenyl) octanoate (mazzeic acid)
	20.45	136,152,151,308,91	308	$C_{18}H_{28}O_4$	Methyl-9-(2,3-dimethoxyphenyl) nonanoate (myakoshic acid)
Substituted dimethoxybenzenes					
	10.46	152,109,137,79,91	152	$C_9H_{12}O_2$	1,2-dimethoxy-4-methyl- benzene (homoveratrole)
	13.22	136,91,151,141,192	192	$C_{12}H_{16}O_2$	1,2-dimethoxy-3-butenylbenzene
	13.34	136,91,152,151,194	194	$C_{12}H_{18}O_2$	1,2-dimethoxy-3-butylbenzene
	14.28	136,151,91,121,206	206	$C_{13}H_{18}O_2$	1,2-dimethoxy-3-pentenylbenzene
	14.34	208,136,151,152,	208	$C_{13}H_{20}O_2$	1,2-dimethoxy-3-pentylbenzene
	15.25	136,151,152,91,121	220	$C_{14}H_{20}O_2$	1,2-dimethoxy-3-hexenylbenzene
	15.31	136,152,137,151,91	222	$C_{14}H_{22}O_2$	1,2-dimethoxy-3-hexylbenzene*
	16.20	136,91,151,152,138	234	$C_{15}H_{22}O_2$	1,2-dimethoxy-3-heptenylbenzene
	16.26	136,236,152,151,91	236	$C_{15}H_{24}O_2$	1,2-dimethoxy-3-heptylbenzene*
	22.45	151,152,136,346,91	346	$C_{23}H_{38}O_2$	1,2-dimethoxy-pentadecenylbenzene ᵗ
	22.57	152,348,151,136,91	348	$C_{23}H_{40}O_2$	1,2-dimethoxy-pentadecylbenzene
Mono- and dicarboxylic fatty acid methyl esters					
	6.96	74,43,59,41,87	130	$C_7H_{14}O_2$	Hexanoic acid, methyl ester
	8.40	74,43,41,87,55	144	$C_8H_{16}O_2$	Heptanoic acid, methyl ester
	9.64	74,55,96,82,41	156	$C_9H_{16}O_2$	4-Octenoic acid, methyl ester
	9.71	74,87,43,41,55	158	$C_9H_{18}O_2$	Octanoic acid, methyl ester
	10.99	74,87,43,41,55	172	$C_{10}H_{20}O_2$	Nonanoic acid, methyl ester
	12.18	74,87,43,41,55	186	$C_{11}H_{22}O_2$	Decanoic acid, methyl ester
	13.59	69,55,74,67,97	202	$C_{10}H_{18}O_4$	Octanedioic acid, dimethyl ester
	14.30	74,87,43,41,55	214	$C_{13}H_{26}O_2$	Dodecanoic acid, methyl ester
	14.57	55,83,74,152,111	216	$C_{11}H_{20}O_4$	Nonanedioic acid, dimethyl ester (azelaic acid methyl ester)

	15.32	74, 87,43,41,55	228	$C_{14}H_{28}O_2$	Tridecanoic acid, methyl ester*
	15.60	74,55,125,98,97	230	$C_{12}H_{22}O_4$	Decanedioic acid, dimethyl ester ‘
	17.16	74,87,43,55,143	256	$C_{16}H_{32}O_2$	Pentadecanoic acid, methyl ester
	18.00	74,87,43,55,41	270	$C_{17}H_{34}O_2$	Hexadecanoic acid, methyl ester (Palmitic acid, methyl ester)
	18.87	74,87,143,41,129	284	$C_{18}H_{36}O_2$	Heptadecanoic acid, methyl ester
	19.61	74,87,43,55,41	298	$C_{19}H_{38}O_2$	Octadecanoic acid, methyl ester (Stearic acid, methyl ester)
	21.28	69,137,71,83,201	NA	NA	NA
	21.60	74,87,43,55,57	340	$C_{22}H_{44}O_2$	Heneicosanoic acid, methyl ester
	23.72	74,87,43,55,57	382	$C_{25}H_{50}O_2$	Tetracosanoic acid, methyl ester

712 * co-elution, t means that only a trace of compounds was detected

713